Spin-Wave Amplification and Lasing Driven by Inhomogeneous Spin-Transfer Torques

R. J. Doornenbal,[1] A. Roldán-Molina,[2] A. S. Nunez,[3] and R. A. Duine[1,4]

[1]*Institute for Theoretical Physics, Utrecht University, Leuvenlaan 4, 3584 CE Utrecht, Netherlands*
[2]*Universidad de Aysn, Calle Obispo Vielmo 62, Coyhaique, Chile*
[3]*Departamento de Física, Facultad de Ciencias Físicas y Matemáticas, Universidad de Chile, Casilla 487-3, Santiago, Chile*
[4]*Department of Applied Physics, Eindhoven University of Technology, P.O. Box 513, 5600 MB Eindhoven, Netherlands*

We show that an inhomogeneity in the spin-transfer torques in a metallic ferromagnet under suitable conditions strongly amplifies incoming spin waves. Moreover, at nonzero temperatures the incoming thermally occupied spin waves will be amplified such that the region with inhomogeneous spin-transfer torques emits spin waves spontaneously, thus constituting a spin-wave laser. We determine the spin-wave scattering amplitudes for a simplified model and setup, and show under which conditions the amplification and lasing occurs. Our results are interpreted in terms of a so-called black-hole laser, and could facilitate the field of magnonics, which aims to utilize spin waves in logic and data-processing devices.

Introduction.—Spin waves are collective excitations in magnetically ordered materials. At the semiclassical level, spin waves in ferromagnets correspond to a wavelike pattern of precessing spins in which the relative phase of the precession of two spatially separated spins is determined by the ratio of their distance to the wavelength of the spin wave. When the exchange interactions dominate, the spin precession is circular. Anisotropies and dipolar interactions, however, generically lead to elliptically precessing—in short, elliptical—spin waves.

Though spin waves are neutral excitations, they are able to transfer angular momentum. Magnonics [1,2] is named after the quasiparticle, the magnon, associated with a spin wave. This field has the ultimate goal of controlling and manipulating spin waves to the point that they can be used to realize energy-efficient data-processing and logic devices. One hurdle to realize technology based on spin waves is that they have a finite lifetime as a result of processes that lead to loss of spin angular momentum and relax the magnetization. Hence, experimental progress has been nearly exclusively made using a unique low magnetic-damping material: the complex magnetic insulator yttrium iron garnet (YIG), thereby limiting the process as it is difficult to fabricate and pattern at high quality in reduced dimensions.

The relaxation of spin waves can be counteracted by injection of spin angular momentum [3,4]. This has been demonstrated in YIG/Pt [5] and Permalloy/Pt-based material systems [6] with electrically driven spin injection via the spin Hall effect [7] and in YIG/Pt with thermally driven spin injection [8,9]. In these examples, the amplitude enhancement of the spin waves is proportional to the applied bias, which may be a limiting factor in case the damping that needs to be overcome is large, or because of the associated heating.

Other proposed mechanisms for the amplification of spin waves involve the interaction of spin waves with electromagnetic [10–14] or magnetoelastic [15] waves. These have the drawback that the input signal is an alternating (ac) signal of which the frequency needs to be matched to that of the spin waves. Moreover, the inductive coupling of spin waves with electromagnetic waves becomes small as devices are miniaturized.

In this Letter, we propose a different way to amplify spin waves. In our proposal the input is a direct current (dc), whereas the frequency of the amplified spin waves can be tuned by appropriate device geometry. Our scheme is well suited for miniaturization as it makes use of the spin-transfer torques that arise in the bulk of ferromagnetic metals as a result of the interaction between the spin-polarized electronic current and the magnetization [16]. The basic setup we consider is sketched in Fig. 1. It consists of a ferromagnetic metallic wire with a constriction. A charge current driven through the wire will have a larger current density in the narrow part of the wire, as compared to the wider parts. As a result, the velocity that characterizes the spin-transfer torques and determines, for example, the current-induced spin-wave Doppler shift [17] will be larger in the narrower part of the wire. For sufficiently large current densities, the Doppler shift will make the spin-wave energies and frequencies in the narrow part of wire negative (indicated in red in Fig. 1), while in the wider parts of the wire they remain positive. Moreover, in the case of a finite spin-wave ellipticity, the spin waves with positive and negative energy are coupled in the regions where the width of the wire changes. As a result of this coupling, spin waves can be created simultaneously in the wide and narrow parts of the wire without changing the total magnetic energy. For the spin-wave modes that bounce back and forth in
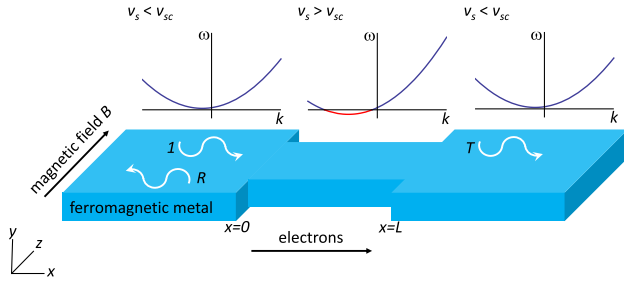
FIG. 1. The setup that is considered in this Letter. A ferromagnetic wire with magnetization saturated in the z direction is subjected to a current density driven in the long direction of the wire. The wire has an indent such that the current density in this narrow region is larger than in the wider parts of the wire. For large enough currents, the resulting current-induced spin-wave Doppler shift pushes the spin-wave energies indicated in red to negative values in the narrow part of the wire while the spin-wave energies in the wide parts of the wire remain positive. The spin-wave frequency ω is sketched as a function of the wave number k in the three different regions.

the narrow part of the wire, the coupling between negative-energy and positive-energy spin waves can be resonant. We show that this leads to an enormous enhancement of the transmission and reflection amplitudes for spin waves that are scattered off the narrow part of the wire and that fulfil the resonance condition. Moreover, this enhancement is so large that the thermally excited spin waves that fulfill the resonance condition will be amplified and emitted from the narrow part of the wire and overwhelm all other spin waves, thus constituting a spin-wave laser.

Model and setup.—We consider a ferromagnetic metal subject to an external field B in the z direction, and charge current $\boldsymbol{j}$. The magnetization direction $\boldsymbol{n}(\boldsymbol{x},t)$ obeys the Landau-Lifshitz-Gilbert equation with spin-transfer torques that is given by [16]

$$(\partial_t + \boldsymbol{v}_s \cdot \nabla)\boldsymbol{n} = \boldsymbol{n} \times \boldsymbol{H}_{\text{eff}} - \alpha \boldsymbol{n} \times \left(\partial_t + \frac{\beta}{\alpha}\boldsymbol{v}_s \cdot \nabla\right)\boldsymbol{n}. \quad (1)$$

This equation describes precession of the magnetization around the effective field $\boldsymbol{H}_{\text{eff}} = -\delta E/\hbar\delta\boldsymbol{n}$, where E is the magnetic energy functional. We consider a generic energy functional that incorporates exchange, anisotropy, and the external field and is given by

$$E = \int \frac{dV}{a^3}\left[-\frac{1}{2}J\boldsymbol{n}\cdot\nabla^2\boldsymbol{n} + \frac{1}{2}K_x n_x^2 + \frac{1}{2}K_y n_y^2 - Bn_z\right]. \quad (2)$$

In this expression, a is the size of the unit cell, J is the exchange constant, and K_x and K_y are anisotropy constants. In case that the anisotropy constants are equal, the spin waves are circular. Because of shape and crystalline anisotropy, the spin wave are typically elliptical, corresponding to the case that $K_x \neq K_y$.

The spin-transfer torques [3,4] in the Landau-Lifshitz-Gilbert equation (1) are characterized by the velocity $\boldsymbol{v}_s = -gP\mu_B\boldsymbol{j}/2eM_s$, which is proportional to the current density and further determined by the current polarization P, the Landé factor g, the Bohr magneton μ_B, the elementary charge e, and the saturation magnetization M_s. The adiabatic spin-transfer torque [18,19] appears on the left-hand side of Eq. (1), whereas the nonadiabatic spin-transfer torque [20,21] appears on the right-hand side and is parametrized by the dimensionless constant $\beta \ll 1$. The Gilbert damping constant $\alpha \ll 1$ determines the rate of decay of the magnetization direction.

We take K_x, K_y, $B > 0$ so that the equilibrium direction of magnetization is the z direction. Linearizing around this equilibrium direction yields the dispersion relation,

$$\omega_{\boldsymbol{k}} - \boldsymbol{v}_s \cdot \boldsymbol{k} = \omega_{\boldsymbol{k}}^0 - i\alpha\omega_{\boldsymbol{k}}^0 - i(\alpha - \beta)\boldsymbol{v}_s \cdot \boldsymbol{k}, \quad (3)$$

with $\hbar\omega_{\boldsymbol{k}}^0 = \sqrt{(\hbar\omega_0)^2 + 2J\hbar\omega_0 k^2 + J^2 k^4 - \Delta^2}$, the real part of the spin-wave dispersion in the absence of current, and where $\hbar\omega_0 \equiv B + (K_x + K_y)/2$ and $\Delta \equiv (K_y - K_x)/2$ and we assumed $\Delta > 0$ without loss of generality. This parameter is to some extent tunable by the wire geometry. In deriving the above dispersion relation, we took $\boldsymbol{v}_s$ constant, but we will drop this assumption shortly.

For $|\boldsymbol{v}_s| > v_{s,c} = \sqrt{2J/\hbar^2}\sqrt{\hbar\omega_0 + \sqrt{(\hbar\omega_0)^2 - \Delta^2}}$, the real part of the dispersion in Eq. (3) becomes negative. This signals an energetic instability as the system may lower its energy by creating negative-energy excitations. From now on, we assume that $\beta \approx \alpha$. This implies that the system remains dynamically stable even when it is energetically unstable, because small-amplitude fluctuations are damped out. This results from the imaginary part of the dispersion relation in Eq. (3), which remains negative when $\beta \approx \alpha$.

In the remainder of this Letter we consider the system sketched in Fig. 1, in which a local increase in the velocity $\boldsymbol{v}_s$ is accomplished by a narrow region in a wire of the metallic ferromagnet. Moreover, we assume that the current density is such that $\boldsymbol{v}_s$ is above the critical value $v_{s,c}$ in the narrow part of the wire, whereas it is below the critical value in the wider parts of the wire. The resulting local spin-wave dispersions are also sketched in Fig. 1 and correspond approximately to shifted parabolas. The negative-energy modes in the narrow part of the wire are indicated by the red dispersion curve.

Scattering solutions.—We now proceed to construct spin-wave scattering solutions to the Landau-Lifshitz-Gilbert equation. We neglect in the first instance the magnetization relaxation and put $\alpha = \beta = 0$. We assume, moreover, that the transverse dimensions of the wire in the y and z direction are very small so that we may drop the dependence of $\boldsymbol{n}$ on y and z, and may, moreover, take $\boldsymbol{v}_s = v_s(x)\hat{x}$. We further assume that the regions where the wire becomes wider and narrower are very small so that we may put $v_s \equiv v_L < v_{s,c}$ independent of x in the wider part
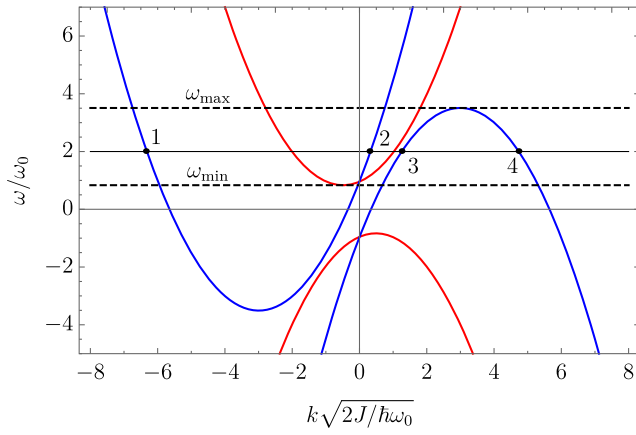
FIG. 2. Dispersion relation for $v_s < v_{s,c}$ (red curves) and $v_s > v_{s,c}$ (blue curves). Black dots mark the four wave numbers corresponding to a generic value $\omega < \omega_{\max}$ in the $v_s > v_{s,c}$ sector. Parameter values are $v_L = 0.5\sqrt{2J\omega_0/\hbar}$, $v_M = 3.0\sqrt{2J\omega_0/\hbar}$, $\Delta = 0.3\hbar\omega_0$.
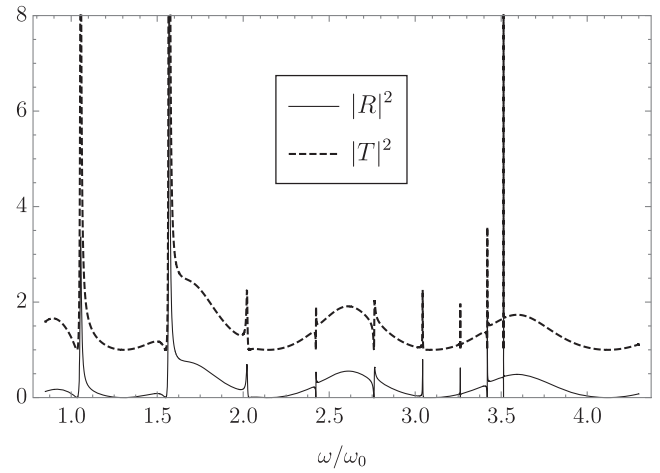

FIG. 3. Transmission (broken line) and reflection (solid line) probabilities off the spin-transfer torque inhomogeneity, see Fig. 1, as a function of spin-wave frequency. Parameter values are $v_L = 0.5\sqrt{2J\omega_0/\hbar}$, $v_M = 3.0\sqrt{2J\omega_0/\hbar}$, $\Delta = 0.7\hbar\omega_0$.

of the wire and $v_s \equiv v_M > v_{s,c}$ independent of x in the narrow part of the wire. We take the narrow part of the wire between $x = 0$ and $x = L$.

To construct the scattering solutions it is convenient to introduce $\psi \equiv n_x - i n_y$. The linearized solutions of the Landau-Lifshitz-Gilbert equation are then given by $\psi(x, t) = u(x)e^{-i\omega t} - v^*(x)e^{i\omega t}$, where the equations for $u(x)$ and $v(x)$ are found from the Landau-Lifshitz-Gilbert equation in Eq. (1). The plane-wave solutions take the form

$$\begin{pmatrix} u(x) \\ v(x) \end{pmatrix} = \begin{pmatrix} F \\ G \end{pmatrix} e^{ikx}, \tag{4}$$

where F, G are complex coefficients. From the equations for $u(x)$ and $v(x)$ we obtain the dispersion relation $(\omega_k - \bm{v}_s \cdot \bm{k})^2 = (\omega_k^0)^2$.

From now on we take $\omega > 0$ without loss of generality. At a given frequency ω, there are in general four (complex) values of k that satisfy the dispersion. These are denoted by k_i, with $i = 1, 2, 3, 4$ and are labeled according to Fig. 2. Different ω regimes need to be distinguished. Firstly, for $v_s < v_{s,c}$, the dispersion exhibits a gap $\omega_{\min}$. We require $\omega \geq \omega_{\min}$ in order for scattering solutions to exist. For the regions where $v_s < v_{s,c}$ there are then two propagating modes with real k and two growing or decaying modes with imaginary k. Secondly, for $v_s > v_{s,c}$, there exists a range of ω from $\omega_{\min}$ to $\omega_{\max}$ within which there exist four real wave vectors k that satisfy the dispersion relation. For ω exceeding $\omega_{\max}$, two of the solutions for k are real and two are imaginary.

In what follows we will look at scattering solutions and hence assume $\omega > \omega_{\min}$. The coefficients of the respective growing modes for $x < 0$ and $x > L$ must vanish. In addition, we impose matching conditions at both jumps

in v_s. The functions $u(x)$ and $v(x)$, as well as their first derivatives, are required to be continuous. This leads to a system of linear equations that can be solved for the reflected and transmitted amplitudes. Here, the reflection amplitude R is defined as the ratio between the F amplitudes [Eq. (4)] of the incoming and reflected wave, whereas the transmission amplitude T is defined as the same ratio but for incoming and transmitted wave. (One could also consider similar ratios of the G amplitudes. This choice does not affect the location of the resonances.)

Results.—In Fig. 3 we show the results for the spin-wave transmission and reflection probabilities as a function of frequency, with the choice $L = 12\sqrt{2J/\hbar\omega_0}$. For distinct frequencies both reflection and transmission are strongly enhanced. We refer to the peaks in the reflection and transmission amplitudes as resonances. We have found that the resonance condition is well approximated by the equation

$$|k_4 - k_3| = \frac{2\pi n}{L} + \mathcal{O}\left(\frac{1}{L^2}\right), \tag{5}$$

where $n = 1, 2, \ldots$. The first term of this equation has the physical interpretation that the counterpropagating waves corresponding to k_3 and k_4 interfere constructively between $x = 0$ and $x = L$. Near $\omega = \omega_{\max}$, the dispersion relation is approximately parabolic. This allows us to describe the resonant frequencies ω_n with the simple approximate formula $\omega_n = \omega_{\max} - n^2\Gamma^2$, where $n = 1, \ldots,$ $\lfloor\sqrt{\omega_{\max} - \omega_{\min}}/\Gamma\rfloor$ and $\Gamma \approx \pi\sqrt{J/\hbar L^2} + \mathcal{O}(1/L^2)$. The value of Γ is only weakly sensitive to the parameters v_L, v_M, Δ. Varying the parameters v_L, v_M affects the location of the resonances significantly only by shifting them all, via a change in the value of $\omega_{\max}$. For $\omega > \omega_{\max}$, there are no resonances at all. This is explained by the fact that the wave
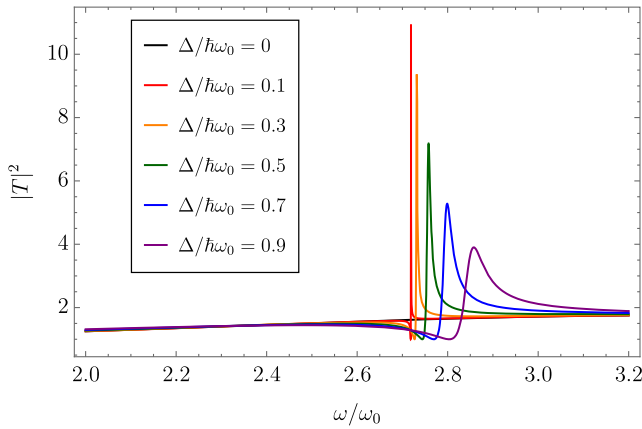
FIG. 4. Transmission probabilities near a resonance, for different Δ. The resonance peak is sharper and higher for small $\Delta > 0$, but is not present if $\Delta = 0$. Parameter values are $v_L = 0.5\sqrt{2J\omega_0/\hbar}$, $v_M = 3.0\sqrt{2J\omega_0/\hbar}$.

vectors k_3, k_4 are complex in this case. In Fig. 4 we have enlarged a single resonance peak for different values of Δ. We find that smaller Δ results in higher and narrower peaks, but no resonances are present if $\Delta = 0$.

Given the strong enhancement of the reflection and transmission amplitudes, the occupation of the incoming spin waves by thermal fluctuations leads to emission of amplified spin waves, thus forming a spin-wave laser. From the condition in Eq. (5) it follows that the resonant frequencies are the same for spin waves incoming from the left and from the right of the constriction. If $1 < \sqrt{\omega_{\max} - \omega_{\min}}/\Gamma < 2$, there is only a single resonance peak. Based on this, one can experimentally engineer a spin-wave laser that emits spin waves at a single frequency.

Discussion and outlook.—Our results can be interpreted as follows. The left transition region, i.e., where v_s changes from $v_s < v_{s,c}$ to $v_s > v_{s,c}$, is a black-hole event horizon for spin waves [22,23] coming in from the left (referring to Fig. 1). The right transition from $v_s > v_{s,c}$ to $v_s < v_{s,c}$ is a white-hole horizon for spin waves coming from the right. Because the spin waves do not disperse linearly, these horizons are referred to as dispersive horizons [24]. In the field of analogue gravity, such a pair of black-hole-like and white-hole-like event horizons, discussed in Ref. [23] for spin waves, is known to be able to give rise to so-called black-hole lasers [25,26], which exhibit the resonant amplification and lasing we have discussed in our specific setup and model. Within this interpretation, the resonant amplification occurs as a result of the constructive interference of particle-hole coupling processes that arises at each horizon. (This particle-hole coupling gives rise to Hawking radiation in the quantum regime [27].) For the system in Fig. 1, the negative-energy modes are the holes, while the particles correspond to positive-energy modes.

The interpretation as a black-hole laser points to some essential ingredients for the spin-wave amplification and lasing. First of all, the negative-frequency and positive-frequency modes need to be coupled. This coupling occurs only for elliptical spin waves because these are a superposition of positive and negative frequencies. Secondly, though we have assumed a steplike current density, our results are more general as any transition where v_s goes from below (or above) to above (or below) $v_{s,c}$ will couple negative-energy and positive-energy modes and thus lead to amplification and lasing. A unique ingredient of magnetic systems is the way the horizons are implemented, i.e., using electric current rather than flow of the spin waves themselves. This gives rise to the nonadiabatic spin-transfer torque, determined by the parameter β, which has no counterpart in other analogue gravity systems. The existence of these nonadiabatic spin-transfer torques is crucial to make the system dynamically stable.

Typical experimentally accessible values are $J \sim 10^{-39}$ Jm^2 and $B/\mu_B \sim K/\mu_B \sim 0.1$–1 T [23], so that $\omega_0 \sim 10$–100 GHz, and the length scale $\sqrt{J/\hbar\omega_0} \sim 10$–100 nm. This means that resonances should be visible for systems in the range $L \sim 10$–1000 nm. For the transverse modes to be frozen out, the transverse size of the device should be roughly 1 order of magnitude smaller than L to have modes propagating in the x direction that have energy well below the first excited transverse standing modes. One concrete but realistic implementation would be a thin film of a few nanometers thick, with a width in the z direction on the order of 100 nm, and $L = 1000$ nm. Note, however, that freezing out the transverse modes is not a necessary ingredient but was only assumed to simplify the computations. While we have in most of our treatment ignored magnetization relaxation (except for requiring that $\beta \approx \alpha$, which is a typical situation), our results remain valid provided the spin-wave coherence length is much longer than L. This translates to the condition that $1/(\alpha k_i) \gg L$. This condition is easily satisfied given that $\alpha \ll 1$. For the abovementioned typical values of anisotropies and external fields, the current density corresponding to $v_{s,c}$ is on the order of 10^{12} A/m^2 [23]. Though large, this current density is reached often, e.g., in experiments using pulsed current-driven domain-wall motion [16]. Moreover, the critical current density may, in principle, be made arbitrarily low by Dzyaloshinskii-Moriya interactions [28].

We have presented a simple setup and model for spin-wave amplification and lasing. We note that the amplification and lasing that we have discussed occurs already within the linear spin-wave approximation. As we have mentioned, the energy of the emitted spin waves is provided by creating negative-energy excitations in the narrow region of the wire. Future research could focus on more accurate modeling of the setup in Fig. 1, including nonlinearities, dipolar interactions, and more complicated current patterns. Recently, numerical results were reported that show spin-wave emission in a similar setup as the one we consider [31]. A direct comparison between these results and ours is postponed to future work.

[1] V. V. Kruglyak, S. O. Demokritov, and D. Grundler, J. Phys. D **43**, 264001 (2010).

[2] A. V. Chumak and H. Schultheiss, J. Phys. D **50**, 300201 (2017).

[3] J. C. Slonczewski, J. Magn. Magn. Mater. **159**, L1 (1996).

[4] L. Berger, Phys. Rev. B **54**, 9353 (1996); J. Appl. Phys. **81**, 4880 (1997).

[5] V. E. Demidov, S. Urazhdin, A. B. Rinkevich, G. Reiss, and S. O. Demokritov, Appl. Phys. Lett. **104**, 152402 (2014).

[6] O. Gladii, M. Collet, K. Garcia-Hernandez, C. Cheng, S. Xavier, P. Bortolotti, V. Cros, Y. Henry, J.-V. Kim, A. Anane, and M. Bailleul, Appl. Phys. Lett. **108**, 202407 (2016).

[7] J. Sinova, S. O. Valenzuela, J. Wunderlich, C. H. Back, and T. Jungwirth, Rev. Mod. Phys. **87**, 1213 (2015).

[8] E. Padrón-Hernández, A. Azevedo, and S. M. Rezende, Phys. Rev. Lett. **107**, 197203 (2011).

[9] K. Uchida, J. Xiao, H. Adachi, J. Ohe, S. Takahashi, J. Ieda, T. Ota, Y. Kajiwara, H. Umezawa, H. Kawai, G. E. W. Bauer, S. Maekawa, and E. Saitoh, Nat. Mater. **9**, 894 (2010).

[10] Yu. Kornyushin, Phys. Status Solidi **41**, 265 (1970).

[11] G. A. Melkov and S. V. Sholom, Zh. Tekh. Fiz. **60**, 118 (1990).

[12] A. F. Kabychenkov, Phys. Solid State **37**, 371 (1995).

[13] B. A. Kalinikos and M. P. Kostylev, IEEE Trans. Magn. **33**, 3445 (1997).

[14] E. Souto, O. A. C. Nunes, D. A. Agrello, and A. L. A. Fonseca, Phys. Lett. A **286**, 353 (2001).

[15] A. Khitun, D. E. Nikonov, and K. L. Wang, J. Appl. Phys. **106**, 123909 (2009).

[16] D. C. Ralph and M. D. Stiles, J. Magn. Magn. Mater. **320**, 1190 (2008).

[17] V. Vlaminck and M. Bailleul, Science **322**, 410 (2008).

[18] Ya. B. Bazaliy, B. A. Jones, and S.-C. Zhang, Phys. Rev. B **57**, R3213 (1998).

[19] J. Fernández-Rossier, M. Braun, A. S. Núñez, and A. H. MacDonald, Phys. Rev. B **69**, 174412 (2004).

[20] G. Tatara and H. Kohno, Phys. Rev. Lett. **92**, 086601 (2004); **96**, 189702 (2006).

[21] S. Zhang and Z. Li, Phys. Rev. Lett. **93**, 127204 (2004).

[22] G. Jannes, P. Maïssa, T. G. Philbin, and G. Rousseaux, Phys. Rev. D **83**, 104028 (2011).

[23] A. Roldán-Molina, A. S. Nunez, and R. A. Duine, Phys. Rev. Lett. **118**, 061301 (2017).

[24] J. Chaline, G. Jannes, P. Maïssa, and G. Rousseaux, in *Analogue Gravity Phenomenology*, edited by D. Faccio *et al.* (Springer, Heidelberg, 2013).

[25] S. Corley and T. D. Jacobson, Phys. Rev. D **59**, 124011 (1999).

[26] J. Steinhauer, Nat. Phys. **10**, 864 (2014).

[27] S. W. Hawking, Nature (London) **248**, 30 (1974); Commun. Math. Phys. **43**, 199 (1975).

[28] Interfacial Dzyaloshinskii-Moriya interactions lead, for the geometry in Fig. 1, to a term Dk_x on the right-hand side of the spin-wave dispersion in Eq. (3) [29]. Here, D characterizes the strength of the Dzyaloshinskii-Moriya interactions. Using this we find that the critical current changes according to $v_{s,c}^{\text{DMI}} = v_{s,c} - D$. The critical current can thus be made vanishingly small when D is enlarged to be just below the value where the magnetic ground state becomes inhomogeneous (corresponding to $v_{s,c}^{\text{DMI}} = 0$). This latter regime has been reached in bulk magnets that lack inversion symmetry and in magnetic multilayers with perpendicular magnetic anisotropy; see, e.g., [30], which may provide a suitable choice of materials for our proposal. In fact, in any magnetic metal that hosts skyrmions or spirals as part of its phase diagram and which is tuned to the field-polarized state would be a candidate material: in these systems the critical current can be made arbitrarily low by tuning the field from the field-polarized state to the phase boundary that separates it from an inhomogeneous state. Note that, in our proposal, the homogeneous ground state remains dynamically stable when the current is so large that $v_s > v_{s,c}^{\text{DMI}}$ because of the condition that $\alpha = \beta$. In systems with interfacial Dzyaloshinskii-Moriya interactions there are, typically, also sizable spin-orbit torques that may further reduce the critical current. Including spin-orbit torques, and considering also the more general situation that $\alpha \neq \beta$, is, in principle, straightforward and is relegated to future work that should be dedicated to guide specific experimental implementations. For now, we remark that magnetic metals with Dzyaloshinskii-Moriya interactions and, in particular, magnetic multilayers offer a large amount of tunability, so that these are promising systems to reduce the critical current while guaranteeing dynamical stability.

[29] J.-H. Moon, S.-M. Seo, K.-J. Lee, K.-W. Kim, J. Ryu, H.-W. Lee, R. D. McMichael, and M. D. Stiles, Phys. Rev. B **88**, 184404 (2013).

[30] S. Woo *et al.*, Nat. Materials **15**, 501 (2016).

[31] M. Dvornik, R. Khymyn, J. Kerman, V. S. Tiberkevich, and A. N. Slavin, Intrinsic generation of propagating spin waves by a magnonic "black hole" in a current-driven nanoconstricted Wire, in *Proceedings of the International Magnetics Conference INTERMAG-18, Singapore, 2018* (2018), Abstract No. HD-10.